Displaced GAD65 amacrine cells of the guinea pig retina are morphologically diverse

YEN-HONG KAO AND PETER STERLING

Department of Neuroscience, University of Pennsylvania School of Medicine, Philadelphia, Pennsylvania 19104-6058

Abstract

The ganglion cell layer of mammalian retina contains numerous amacrine cells. Many belong to one type, the cholinergic starburst cell, but the other types have not been systematically identified. Using a new method to target sparsely represented cell types, we filled about 200 amacrine neurons in the ganglion cell layer of the guinea pig visual streak and identified 11 types. Ten of these resemble types identified in other species with somas in the inner nuclear layer, but one type has not been previously reported. Most of the types and nearly all the injected cells (95%) arborized low in the synaptic layer where they would co-stratify with various classes of ON ganglion cell. The displaced somas (7% of all amacrine cells) thus represent a heterogeneous pool, which are relatively accessible for study of their interactions with ON ganglion cells.

Keywords: Retina, Amacrine cell, Displaced amacrine, Guinea pig

Introduction

Amacrine somas form a continuous tier at the inner margin of the inner nuclear layer. However, some cells are displaced to the ganglion cell layer (Vaney et al., 1981; Hughes & Wieniawa-Narkiewicz, 1980; Perry & Walker, 1980). Although the main amacrine population is well characterized and known to comprise many different types (MacNeil & Masland, 1998; Vaney, 1991), the morphology of displaced cells has not been systematically studied. One would like particularly to know whether the displaced cells represent novel types absent from the main amacrine layer, or rather if they belong mostly to types previously identified in the main layer.

We studied this question in the visual streak of the guinea pig retina, the species where we had previously identified functional mechanisms that involve spiking amacrine cells (Demb et al., 1999). To start we simply injected many displaced cells with fluorescent dye and then captured their arbors in the synaptic layer. Most proved to be ON starburst cells, which were already known to arborize near the ganglion cell layer (Tauchi & Masland, 1984; Vaney, 1984). Because this preponderance of starburst cells impeded our identifying rarer types, we targeted a specific class of displaced cells by immunostaining for GAD$_{65}$. This identified a large subset of non-starburst cells, which were then injected with diI (Kao & Sterling, 2003). This identified 10 additional types,

most of which are familiar, from the amacrine layer of other species. A recent study in ferret of displaced amacrine cells encountered few starburst cells but, in agreement with the present work, found considerable heterogeneity in their physiology and morphology (Aboelela & Robinson, 2004).

Materials and methods

Tissue preparation

Our studies employed the visual streak of retina from 20 adult guinea pigs. Each animal was deeply anesthetized with 100 mg/kg ketamine, 20 mg/kg xylazine, and 50 mg/kg pentobarbital. Following enucleation, the animal was sacrificed by overdose of pentobarbital. These procedures were performed in accordance with guidelines of University of Pennsylvania and National Institutes of Health. The retina was detached from the pigment epithelium, mounted on a membrane filter (type HA, Millipore, Bedford, MA), then fixed in a solution prepared from 4% paraformaldehyde in 0.1 M phosphate buffer at pH 7.4 for 15–30 min, and stored in 0.1 M phosphate buffer pH 7.4 at 4°C.

Immunostaining

A piece of retina was incubated overnight at 4°C in 0.1 M phosphate buffer pH 7.4, containing GAD$_{65}$ antibody (1:20, Developmental Studies Hybridoma Bank, University of Iowa, IA), 0.3% Tween 20 detergent (Lukas et al., 1998), and 10% normal goat serum. The tissue was washed 3 × 10 min in 0.1 M phosphate

Address correspondence and reprint requests to: Peter Sterling, University of Pennsylvania, Department of Neuroscience, 123 Anatomy/Chemistry Building, Philadelphia, PA 19104-6058. E-mail: peter@retina.anatomy.upenn.edu

buffer and then incubated for 30 min with 1% anti-mouse Alexa-488 (Molecular Probes) or 1% anti-mouse CY3 (Jackson ImmunoResearch, West Grove, PA), and 0.3% Tween 20. To stain all somas, the retina was immersed for 3 min. in 0.1% solution of the nucleic acid dye, SYTO13 (Molecular Probes, Carlsbad, CA), in 0.1M phosphate buffer pH 7.4.

For ChAT (1:100, Chemicon International, Temecula, CA) immunostaining, a piece of retina was incubated for 48 h at 4°C in 0.1 M phosphate buffer pH 7.4, containing 0.5% Triton X-100, and 6% normal goat serum. The tissue was washed 3×10 min in 0.1 M phosphate buffer, and then incubated for 2 h with 1% anti-rabbit rhodamine (Jackson ImmunoResearch) and 0.5% Triton X-100 in 0.1 M phosphate buffer pH 7.4, at room temperature.

The specificity of both antibodies had been established in many previous studies (Kao et al., 2004).

Electrodes and dye solutions

Sharp microelectrodes were pulled from borosilicate glass capillaries to ~30 MΩ (measured with 1 M KCl). The electrode tip was filled with 1% DiI in 100% ethanol, or 1% DiO in methylene chloride. The shank was then filled with 100% ethanol. Dye was expelled by 1–50 nA positive current for 10–20 s.

Microscopy

Injected cells were imaged by confocal microscopy with a ×40 oil immersion objective ($NA = 1.25$) and 1-μm steps in the Z-axis. To prevent tissue shrinkage, the retina was kept moist with 0.1 M phosphate buffer; and to prevent compression, a spacer (~200 μm) was placed between slide and coverslip. The outer boundary of the inner plexiform layer (IPL; 0%) was defined as the junction between the inner nuclear layer (INL) and IPL; the inner margin of the IPL (100%) was defined as the junction of the IPL and the ganglion cell somas. Dendritic stratification is given as the normalized distance between these two boundaries. Cells were drawn from Z-stacks of confocal images.

Results

Number of amacrine cells

By staining with a nucleic acid dye and counting all cells in optical sections through the amacrine tier in the inner nuclear layer, we determined the density of amacrine cells in that layer. We counted five regions (250×250 μm) from two animals for a total of ~6250 cells. The result was 19710 ± 550 cells/mm^2 (mean ± SD; Fig. 1A), similar to the rabbit (Strettoi & Masland, 1996).

The same procedure applied to the ganglion cell layer yielded 2914 ± 260 cells/mm^2, including ganglion and amacrine cells. Ganglion cell bodies were identified by their larger size (>10-μm diameter) and especially by their nuclei located eccentrically; whereas amacrine cell bodies were smaller (≤10-μm diameter) with nuclei located centrally (Fig. 1B). These simple criteria were confirmed by dye-injecting numerous cells and finding that the larger cells with eccentric nuclei always sent an axon into the nerve fiber layer; whereas the smaller cells with central nuclei confined their processes to the inner plexiform layer. Ganglion cell density was 1537 ± 137 cells/mm^2, and displaced amacrine density was 1468 ± 28 cells/mm^2 ($n = 5$). This agrees with the identification of ganglion cells by retrograde labeling (Do-Nascimento et al., 1991). Thus, displaced amacrine cells in guinea pig retina comprise about half of the neurons in the ganglion cell layer and about 7% of all amacrine cells ($6.9 \pm 0.3\%$; $n = 5$).

Identifying types of displaced amacrine cell

We initially injected 100 displaced amacrine cells and most showed the ON starburst morphology: symmetrically radiate dendrites restricted to a narrow stratum of the inner synaptic layer (Fig. 2;
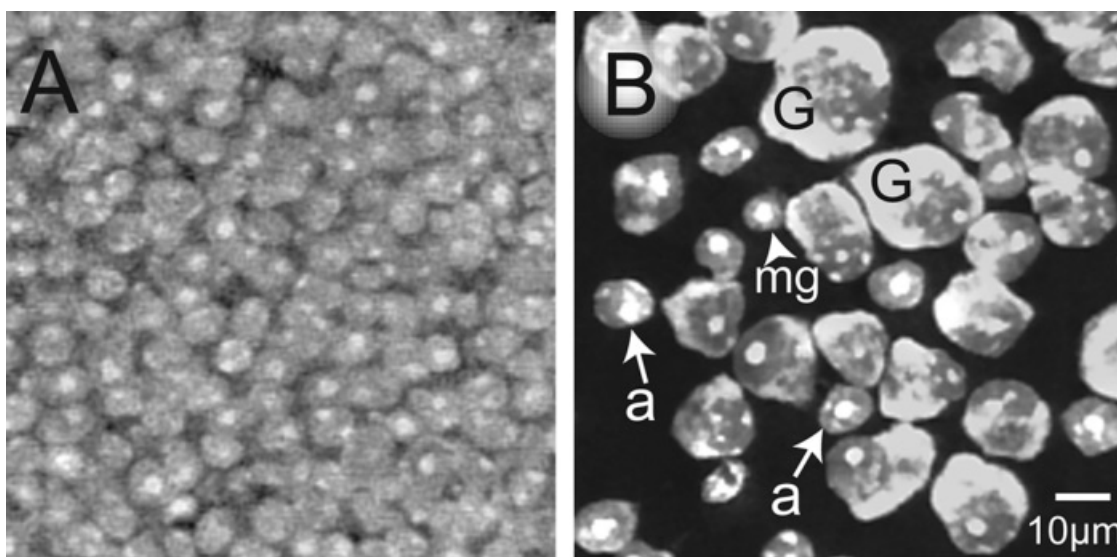

Fig. 1. Displaced amacrine cells comprise 7% of all amacrine cells. (**A**) Somas are confluent in the inner tier of the middle cellular layer, with a density of ~20,000 amacrine cells/mm^2. (Nucleic acid stain). (**B**) Somas are nonconfluent in the ganglion cell layer. Ganglion cells (G) are identified by larger size and eccentric nucleus; amacrine cells (a; arrows) are identified by intermediate size and central nucleus; microglia (mg; arrowhead) are smaller and sparser. These identifications were confirmed by intracellular dye injection. Displaced amacrine cells had a density of ~1500/mm^2. Confocal images, ×40 objectives, 1.25 NA.
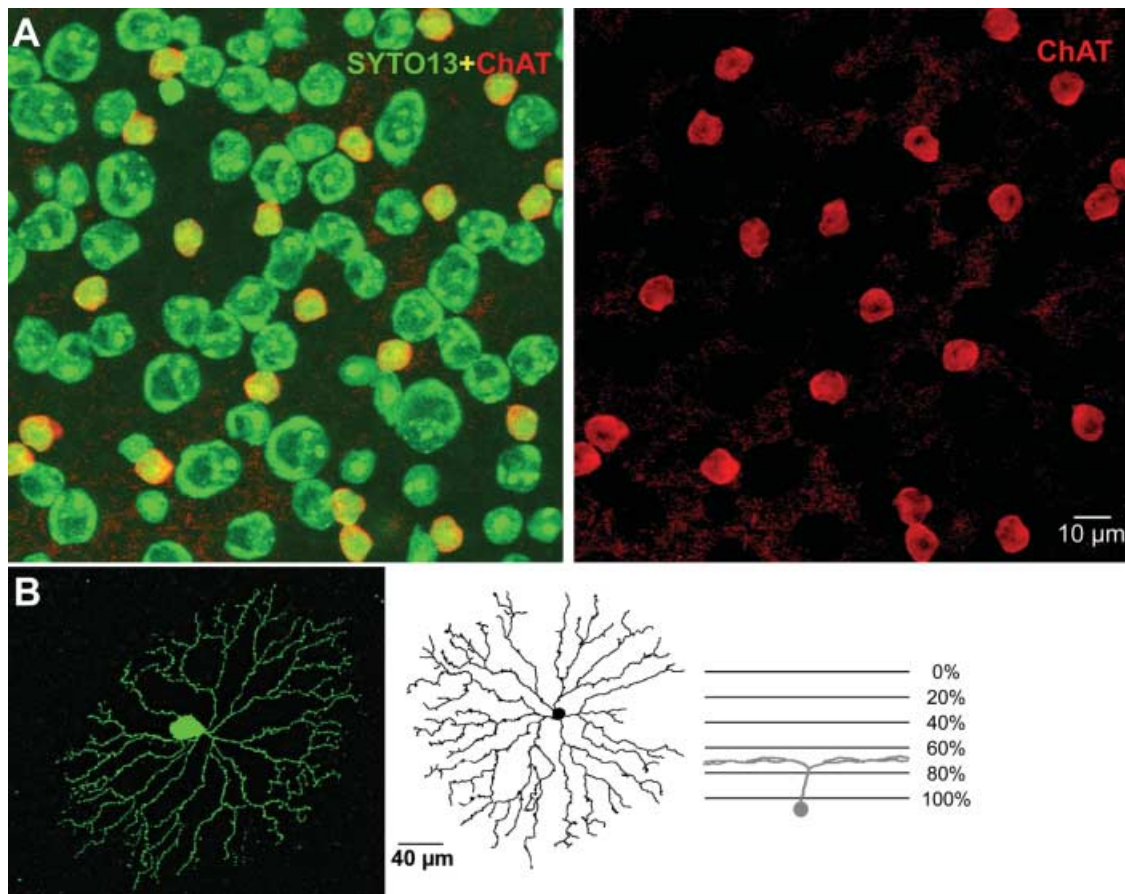
Fig. 2. More than half of the displaced amacrines are ON starburst cells. (**A**) Ganglion cell layer contains 38 displaced amacrine cells, and 21 of these are ChAT-positive. (**B**) ChAT-positive cells show the starburst morphology, the planar dendrites stratify at 70% depth in the synaptic in the IPL. Left, fluorescent image; right, tracing of a different cell.

Tauchi & Masland, 1984; Vaney, 1984). Because the starburst cell is cholinergic (Hayden et al., 1980), we could quantify its distribution by counting displaced cells immunopositive for choline acetyltransferase (ChAT). ChAT-positive somas comprised about half of all displaced cells ($55 \pm 2\%$; $n = 7$; Fig. 2). As anticipated from the cited studies, these displaced starburst somas restricted their processes to the lower half of the inner plexiform layer.

Because most intracellular injections yielded starburst cells, it was difficult to find the others; to address this we immunostained for GAD_{65}. This isoform of glutamic acid decarboxylase did not colocalize with ChAT and thus was absent from starburst cells (Fig. 3). Rather it identified an additional component of the displaced population, comprising 17%. Targeting these (Kao & Sterling, 2003), we successfully filled 96 cells and classified them by dendritic morphology, extent, and stratification.

Types of GAD_{65} cell

The population of GAD_{65}-positive displaced amacrine (DA) cells comprised 10 types, described here from most to least commonly encountered. DA1 stratified narrowly at the $\sim$80% level of the inner plexiform layer, the field of processes spanned 300–400 μm (Fig. 4). The processes distributed asymmetrically, especially compared to the starburst cell (Fig. 2). DA1 comprised $\sim$40% of the injected GAD_{65} cells.

DA2 stratified at the 95% level, just above the ganglion cell layer, with an occasional dendrite straying up to 40% or even up to 20%. The dendritic field spanned $\sim$250–350 μm (Fig. 5). The soma was $\sim$9–10 μm in diameter (*vs.* $\sim$8 μm for the other cell types) and radiated straight dendrites with prominent varicosities ($\sim$1 μm diameter; Fig. 5). DA2 comprised 16% of the injected GAD_{65} cells.

DA3 arborized at two levels of the synaptic layer, mainly at 90% and 10%. The dendritic field spanned about 250–350 μm and like DA1, the dendrites distributed asymmetrically (Fig. 6). The deep dendrites were thicker, straighter, and non-varicose; whereas the superficial dendrites were thinner, curvy, and highly varicose (Fig. 6). DA3 comprised 13% of the injected GAD_{65} cells.

DA4 stratified mainly around 70%, with dendritic fields that spanned from $\sim$ 250–400 μm. Some examples showed one dendrite extending $\sim$150 μm, beyond the others (Fig. 7). DA4 comprised 13% of the injected GAD_{65} cells.

The remaining types, DA5-10, together comprised $\sim$15% of the injected GAD_{65} cells. Although there were only one or a few of each type, they were well stained and clearly differed from the other types. DA5 was medium-field with dendrites that spanned $\sim$150–200 μm. These distributed diffusely at levels between 50% and 90% (Fig. 7). DA6 was wide field, stratifying at 80%. The dendritic field spanned $\sim$600–700 μm (Fig. 7). DA6 resembled DA2 but was three-fold larger.
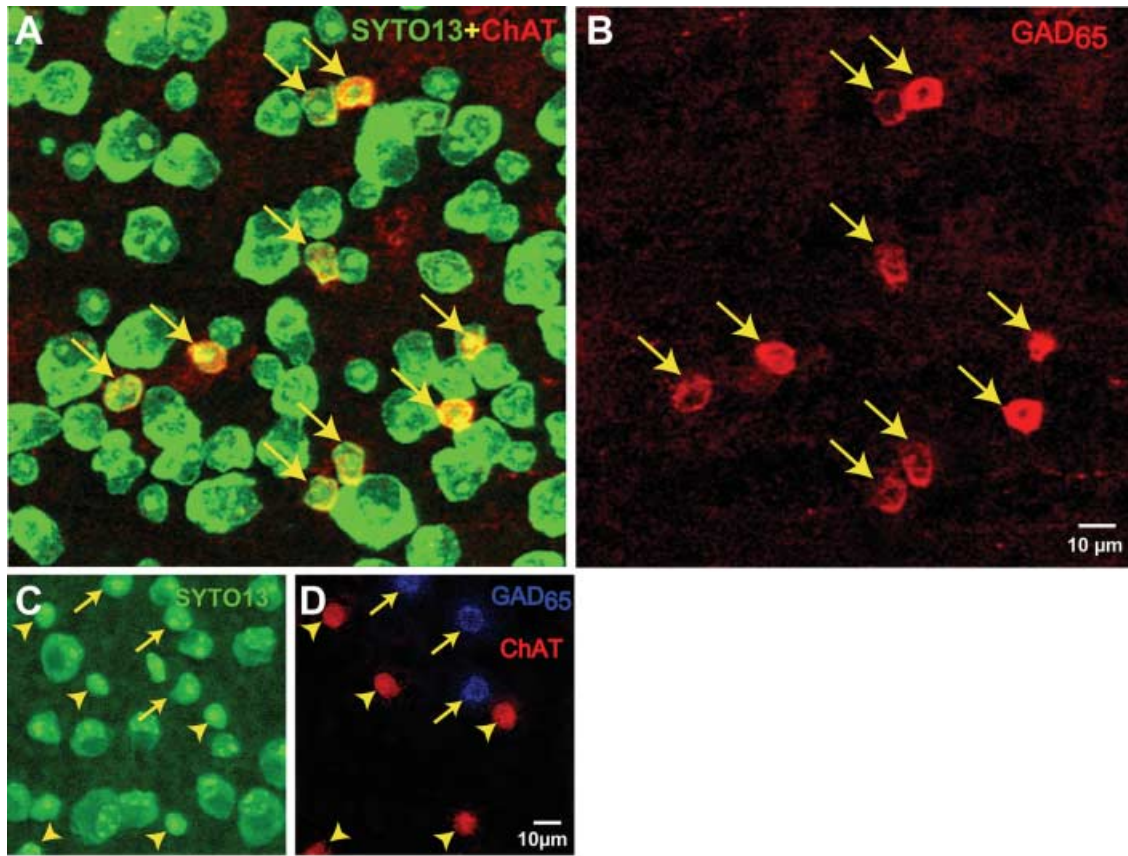
Fig. 3. Certain displaced amacrine cells express GAD$_{65}$. (**A**) Nucleic acid stain shows all the neuron somas in the ganglion cell layer. About half are amacrine cells (see Fig 1B). (**B**) Of 22 displaced cells, nine were GAD$_{65}$-positive (arrows). (**C**) Displaced GAD$_{65}$ cells (arrows) were negative for ChAT, and ChAT cells (arrowheads) were negative for GAD$_{65}$.
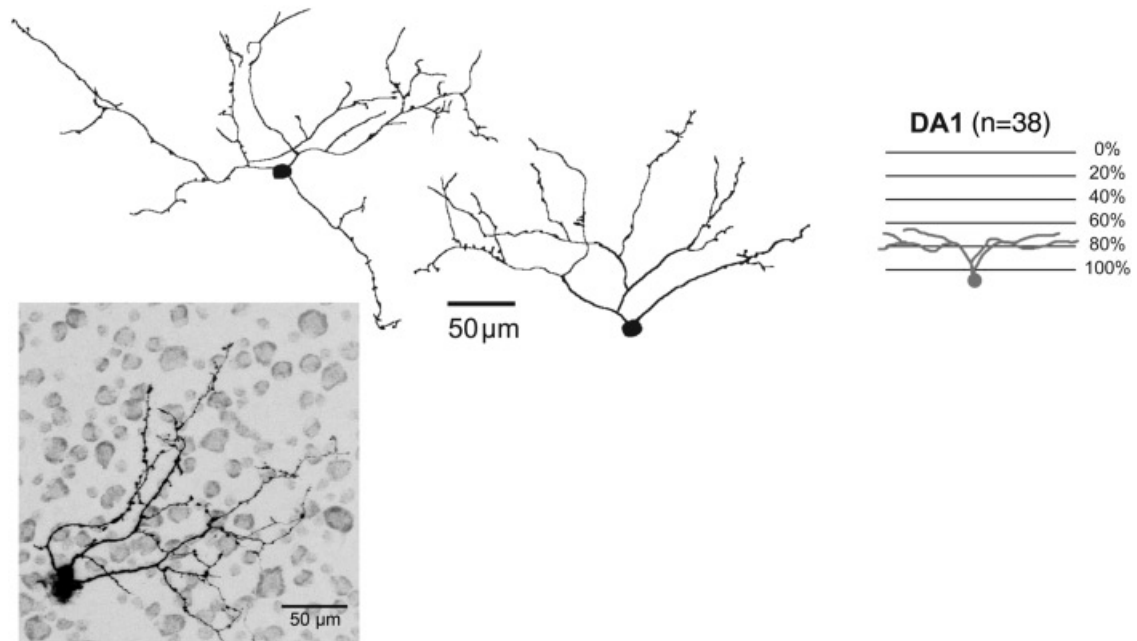

Fig. 4. DA1: Medium dendritic field stratifies narrowly at ~80%. Upper, tracings from fluorescent images. Lower, fluorescent image of a different cell. In this and subsequent figure the schematic drawings illustrate stratification level and omit the distal dendritic segments
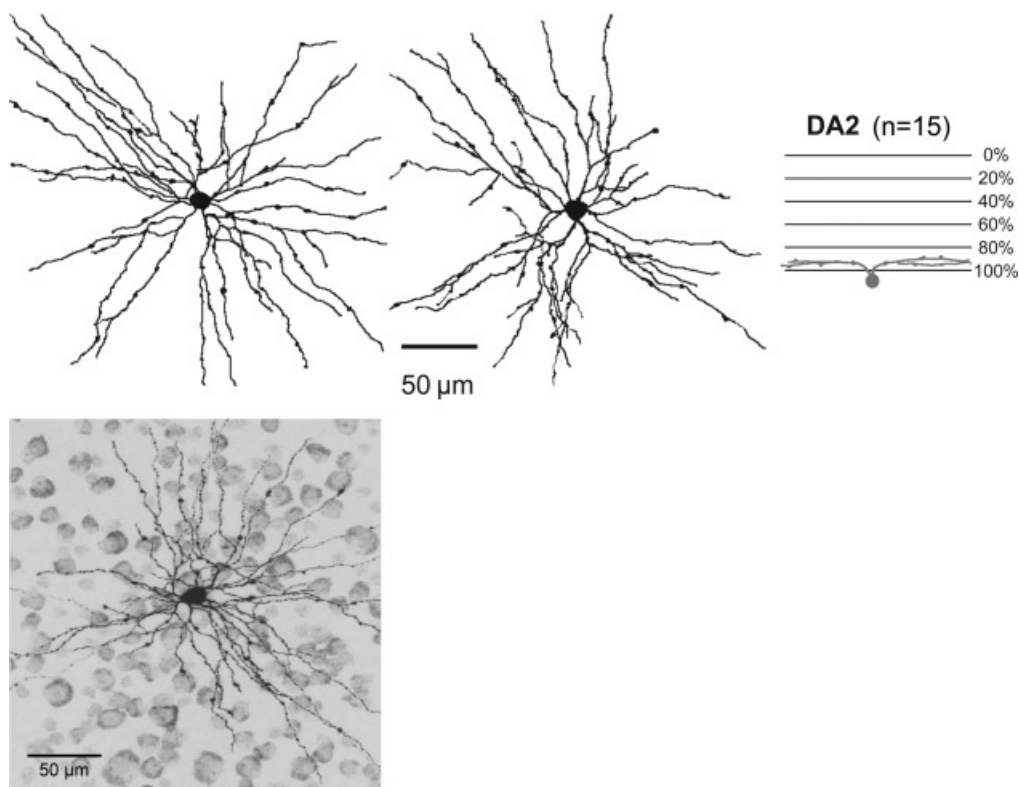
Fig. 5. DA2: Medium dendritic field stratifies at ~95%; Upper, tracings; lower, fluorescent image of a different cell.
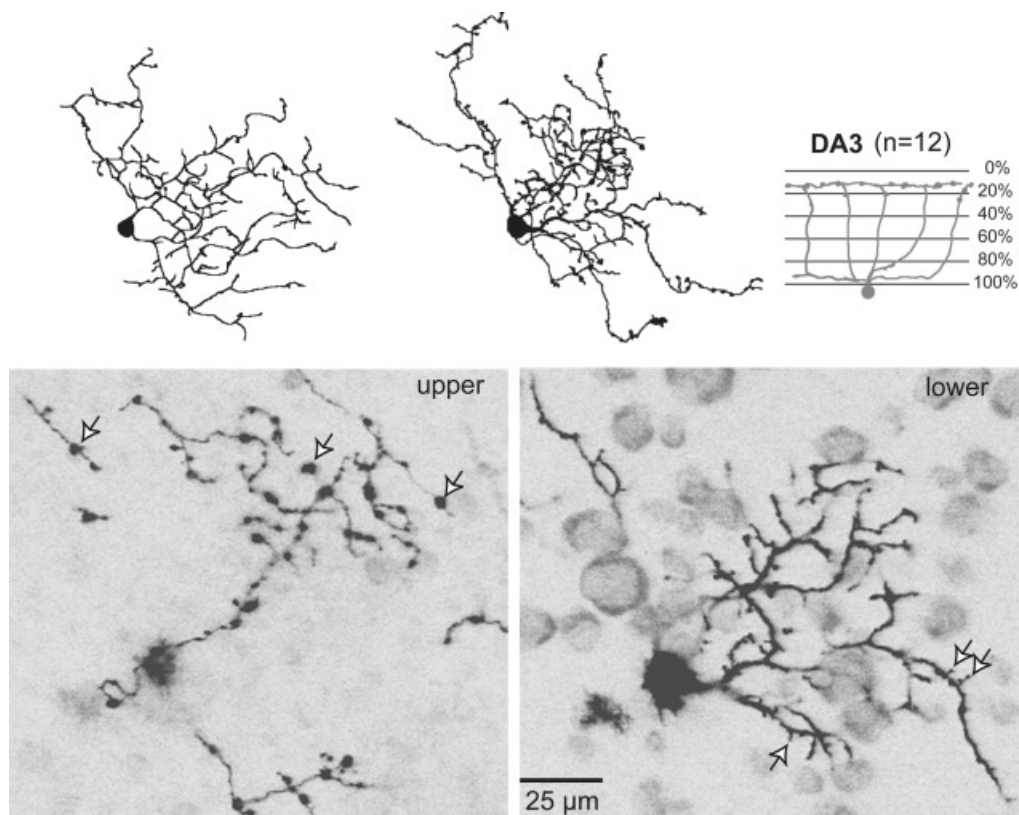

Fig. 6. DA3: Medium dendritic field stratifies at 90 and 10%. Upper and lower arbors express different morphology: upper dendrites are markedly varicose (arrows, lower left); whereas lower dendrites are thick and spiny (arrows, lower right). Upper, tracings; lower, fluorescent images of upper right cell.
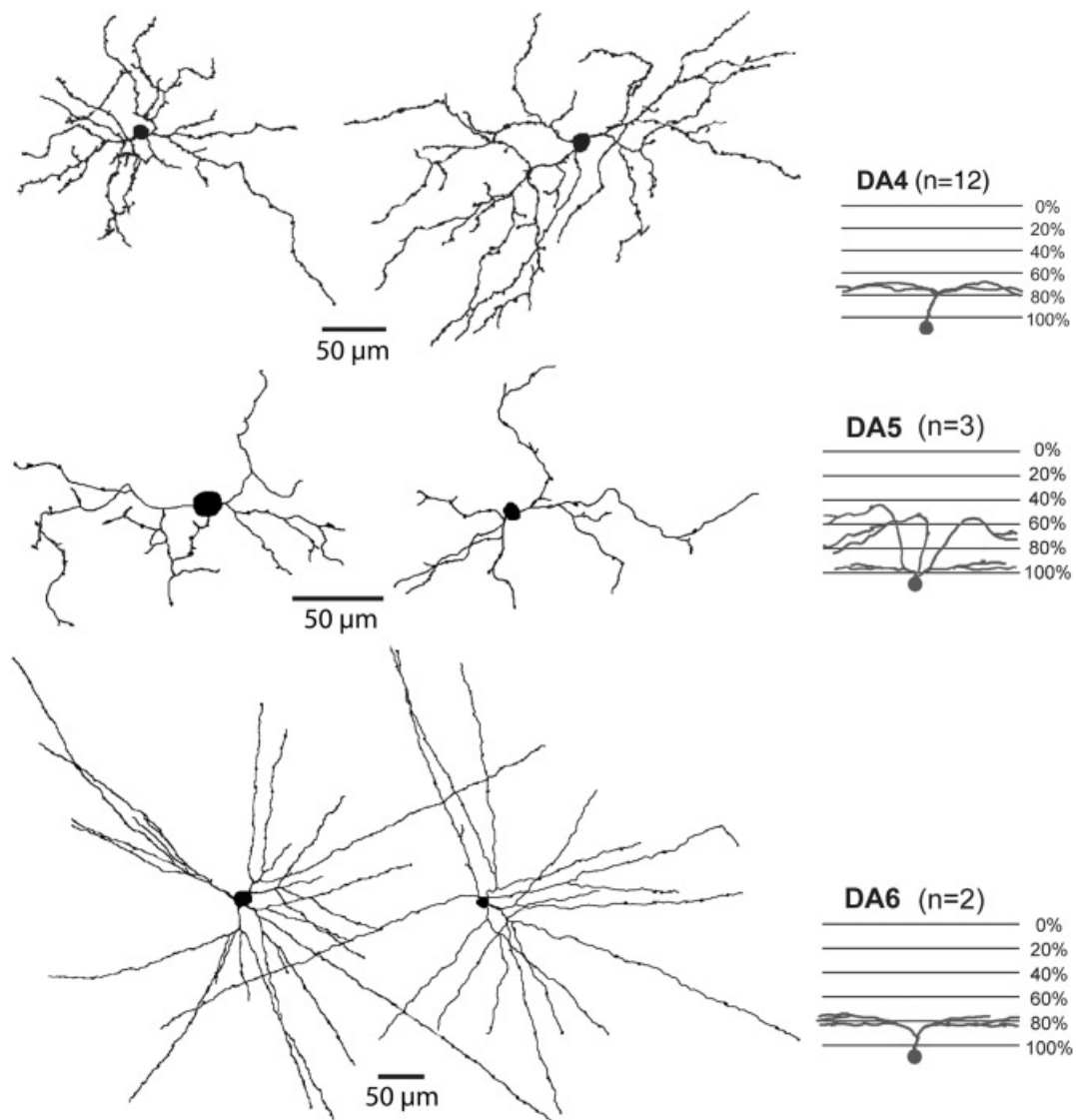
Fig. 7. DA4: Medium dendritic field stratifies at 70%. DA5: Medium dendritic field stratifies diffusely between ~50 and 90%. DA6: Wide dendritic field stratifies narrowly at ~80%.

DA7 was a "long-range" cell (West, 1976). The soma produced one primary process that ascended to ~30% where it branched into local dendrites and several long, straight axons that extended for a millimeter or more (Fig. 8). DA8 was wide-field with dendrites stratified at 30~40% and spanned about 900 μm (Fig. 9). DA9 stratified at 5% (Fig. 10). DA10 was a narrow-field cell, arborizing at 45% and spanned less than 100 μm (Fig. 10).

A plot of stratification *versus* dendritic span separated the cells into numerous distinct clusters (Fig. 11A; see Rodieck & Brening, 1983; Cohen & Sterling, 1990). In several cases two cell types shared the same cluster; for example, the starburst cell plus DA4 and DA2 plus the deep dendrites of DA3. However, other morphological features unambiguously resolved the cluster into two types. Thus the starburst cell is radially symmetrical, but DA4 is irregular and asymmetrical (cf. Figs. 3 and 4). And DA2 is monostratified, whereas DA3 is bistratified. Most of the key distinctions are captured in Fig. 11B.
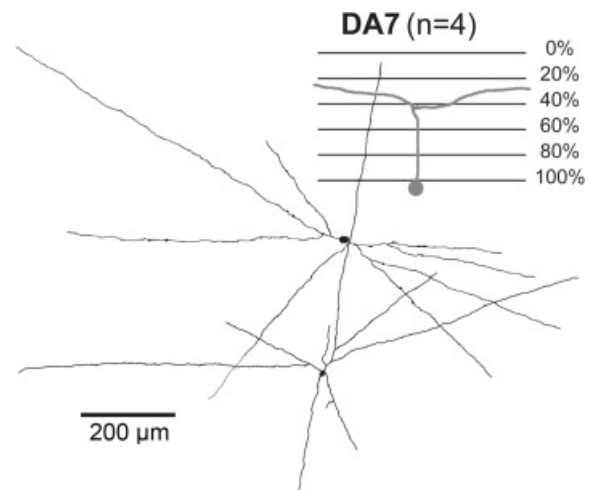

Fig. 8. DA7: long-range cell with multiple axons that travel >1 mm and stratifies at ~30%.
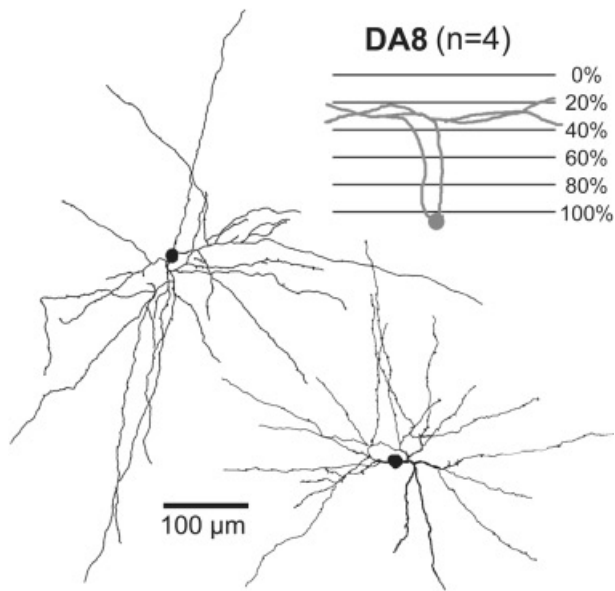
Fig. 9. A8: wide-field cell stratifies at 30–40%.

Discussion

Displaced amacrine cells are diverse.

The displaced amacrine cells identified here are quite diverse, comprising 11 types (Fig 11B; see also Aboelela & Robinson, 2004). The inventory, including cells positive for ChAT (55%) and GAD_{65} (17%), accounts for 72% of all displaced cells. The remainder must include types that synthesize GABA *via* the GAD_{67} isoform and types that use glycine (Andrade da Costa & Hokoc, 2003; Vardi & Auerbach, 1995; Pourcho & Owczarzak, 1991; Pourcho & Goebel, 1987). We were unable to study these types by immuno-targeting because the available antibodies required conditions unsuited for subsequent diI staining. One expects that, when these classes are targeted (perhaps by a virally mediated GFP), they will reveal additional diversity.

Most of the injected cells aborized in the ON strata. This was found for the all of the displaced starburst cells, which were the most numerous, but it was also found for 90% of the GAD_{65} neurons, including 7 of the 10 types (Fig 11A). One of these types (DA3) arborized in outer (10%) and inner (90%) levels of the synaptic layer. If the selectivity noticed here for the ON strata extends to the unstudied 28% of the displaced amacrine population, then it might support the idea that displaced cells are selective for the ON strata—as predicted by Vaney et al. (1981). This would be consistent with the rules governing brain circuitry that generally places cells and whole functional "areas" as close as possible to their targets of connection (Klyachko & Stevens, 2003; Cherniak, 1994). Selective displacement, if present, would also minimize the need for developing processes to navigate past irrelevant targets (Raper, 2000).

Certain amacrine types may be exclusively displaced; that is, present only in the ganglion cell layer. This includes the ON starburst cell (Fig. 2) and possibly DA1 and DA4 because the equivalent types in the cat (A11, A15) are usually displaced (Kolb et al., 1981); also a comprehensive survey in the rabbit found none of these types in the amacrine layer (MacNeil et al., 1999). However, types that contribute equally to both upper and lower levels apparently place their somas in either layer. For example, the A2 soma, whose arbor spans the whole synaptic layer, is mostly in the amacrine layer, but in the cat it is sometimes displaced (Vaney, 1985; Nelson, 1982). This type, being glycinergic, was not targeted in our experiments.

Amacrine types are apparently conserved across species

Bipolar and ganglion cell types are clearly conserved across mammalian species (Sterling, 2004; Masland, 2001). Certain types of amacrine cell are also known to be conserved, such as the A2, starburst, and dopamine cells (Vaney, 1990). However, the amacrine cells are so diverse and relatively unexplored that it remains
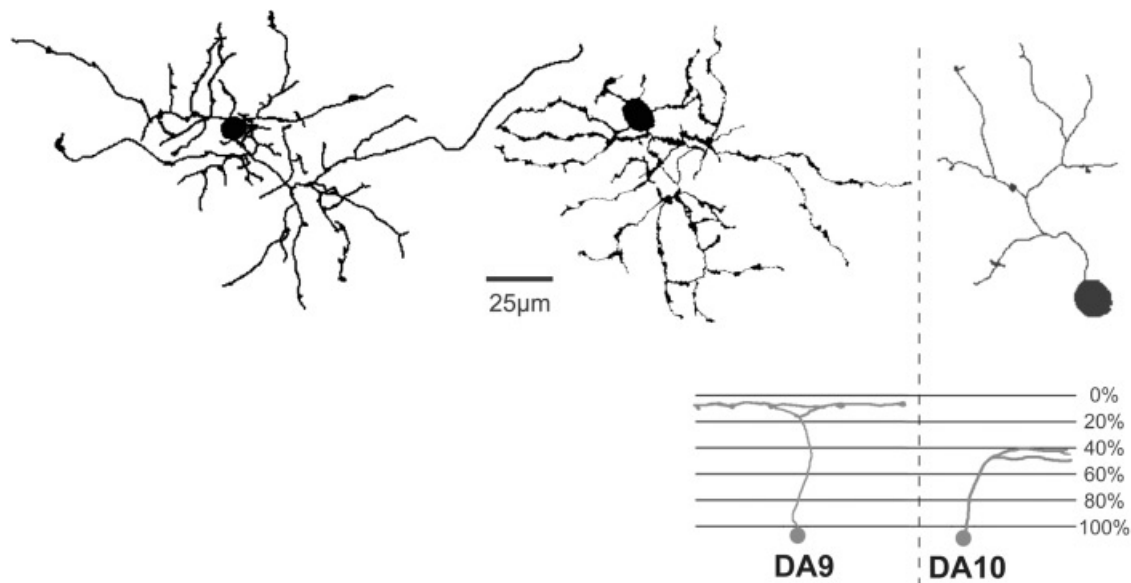

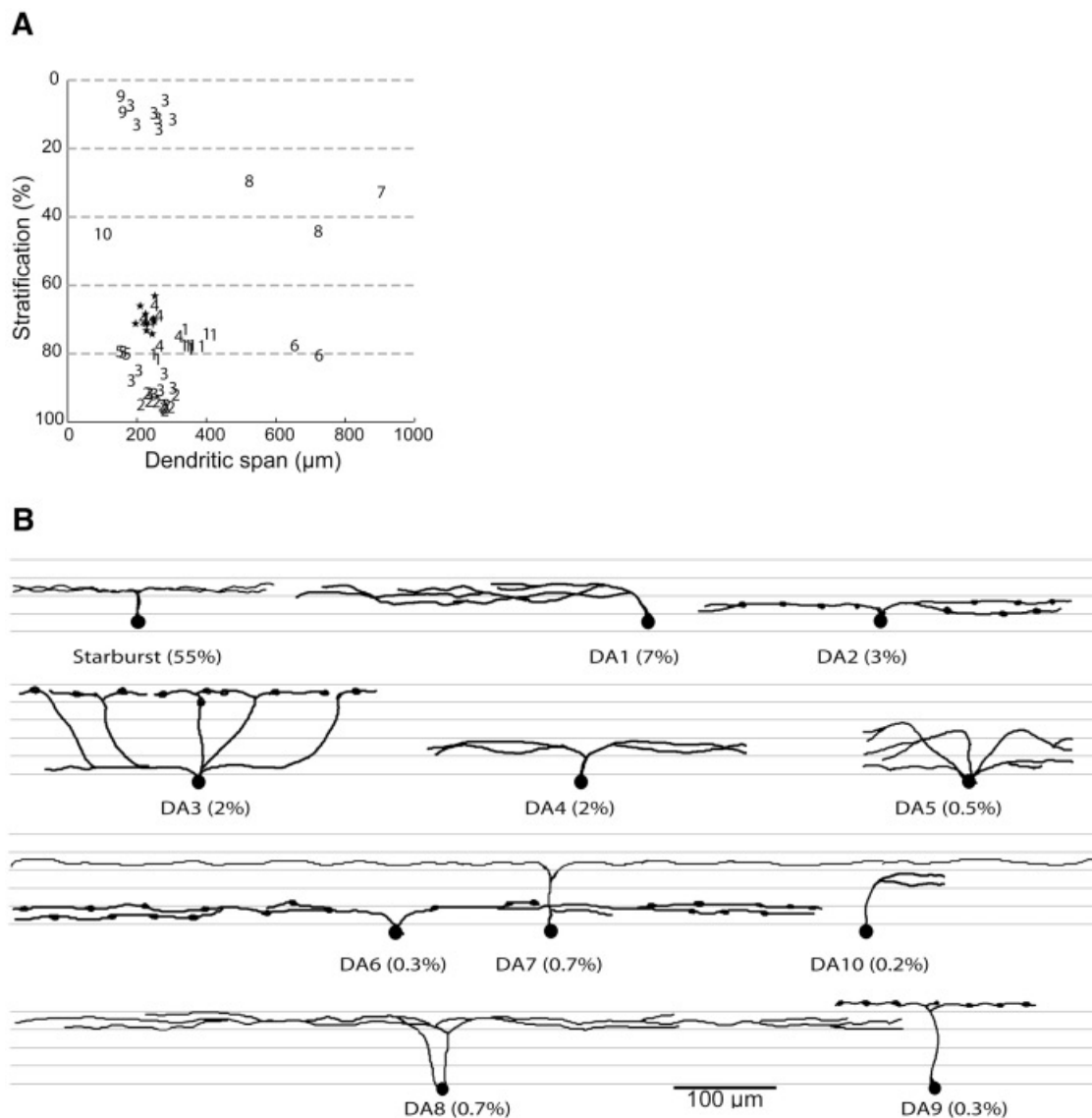**Fig. 10.** DA9 stratifies narrowly at 5%. DA10 stratifies at 45%.

Fig. 11. (**A**) Scatter plot separates most cells into distinct clusters. Numbers represent types summarized in the diagram. In the few cases of overlap (*e.g.*, starburst [⋆] and DA4), the types are easily separated by differences in morphology (cf. Figs. 2, 7) (**B**) Morphology of identified types. Percentages indicate frequency with which each type was encountered.

to determine how completely they are conserved (MacNeil et al., 1999).

Most of the 10 types of GAD_{65} amacrine cell identified here in guinea pig retina do correspond to types identified in other species. DA1, with its asymmetrical dendritic field, resembles cat types A11 and A15; and DA4 resembles cat A14 (Kolb et al., 1981). DA2 and DA6 correspond, respectively, to types S2 and S1 in the rabbit and A17 in the cat (Kolb et al., 1981), which connect reciprocally with the rod bipolar axon terminal (Zhang et al., 2002; Sandell & Masland, 1986). DA3, with its varicose outer processes and fine inner processes, resembles the "fountain" cell in the rabbit (Wright & Vaney, 2000; MacNeil et al., 1999) and the mouse (Tsukamoto, unpublished). DA7 and DA8 correspond, respectively, to the polyaxonal and wide-field amacrine cells in the rabbit (Völgyi et al., 2001; MacNeil et al., 1999). DA9 (narrowly stratified, medium-field) corresponds to the "narrow S1" type in the rabbit (Zhang et al., 2002; Sandell

& Masland, 1986). Only DA5 could not be matched to a known type, which may reflect incomplete knowledge of other species rather than lack of conservation. Incomplete staining cannot explain this unknown type, because our DiI staining labeled thin processes over a millimeter or more. The apparent conservation among amacrine types seems to bolster the idea that circuits in mammalian retina follow a "fundamental plan" (Masland, 2001; Sterling, 2004).

References

ABOELELA, S.W. & ROBINSON, D.W. (2004). Physiological response properties of displaced amacrine cells of the adult ferret retina. *Visual Neuroscience* **21**, 135–144.

ANDRADE DA COSTA, B.L. & HOKOC, J.N. (2003). Coexistence of GAD-65 and GAD-67 with tyrosine hydroxylase and nitric oxide synthase in amacrine and interplexiform cells of the primate, Cebus apella. *Visual Neuroscience* **20**, 153–163.

CHERNIAK, C. (1994). Component placement optimization in the brain. *Journal of Neuroscience* **14**, 2418–2427.

COHEN, E. & STERLING, P. (1990). Demonstration of cell types among cone bipolar neurons of cat retina. *Philosophical Transactions of the Royal Society (London) B* **330**, 305–321.

DEMB, J.B., HAARSMA, L., FREED, M.A. & STERLING, P. (1999). Functional circuitry of the retinal ganglion cell's nonlinear receptive field. *Journal of Neuroscience* **19**, 9756–9767.

DO-NASCIMENTO, J.L.M., DO-NASCIMENTO, R.S.V., DAMASCENO, B.A. & SILVEIRA, L.C.L. (1991). The neurons of the retinal ganglion cell layer of the guinea pig: Quantitative analysis of their distribution and size. *Brazilian Journal of Medical Biological Research* **24**, 199–214.

HAYDEN, S.A., MILLS, J.W. & MASLAND, R.M. (1980). Acetylcholine synthesis by displaced amacrine cells. *Science* **210**, 435–437.

HUGHES, A. & WIENIAWA-NARKIEWICZ, E. (1980). A newly identified population of presumptive microneurones in the cat retinal ganglion cell layer. *Nature* **284**, 468–470.

KAO, Y.-H., LASSOVÁ, L., STERLING, P. & VARDI, N. (2004). Evidence that two types of retinal bipolar cell use both glutamate and GABA. *Journal of Comparative Neurology* **478**, 207–218.

KAO, Y.-H. & STERLING, P. (2003). Matching neural morphology to molecular expression: Single cell injection following immunostaining. *Journal of Neurocytology* **89**, 2360–2369.

KLYACHKO, V.A. & STEVENS, C.F. (2003). Connectivity optimization and the positioning of cortical areas. *Proceedings of the National Academy of Sciences USA* **100**, 7937–7941.

KOLB, H., NELSON, R. & MARIANI, A. (1981). Amacrine cells, bipolar cells and ganglion cells of the cat retina: A Golgi study. *Vision Research* **21**, 1081–1114.

LUKAS, J.R., AIGNER, M., DENK, M., HEINZL, H., BURIAN, M. & MAYR, R. (1998). Carbocyanine postmortem neuronal tracing. Influence of different parameters on tracing distance and combination with immunocytochemistry. *Journal of Histochemistry & Cytochemistry* **46**, 901–910.

MACNEIL, M.A., HEUSSY, J.K., DACHEUX, R.F., RAVIOLA, E. & MASLAND, R.H. (1999). The shapes and numbers of amacrine cells; matching of photofilled with golgi-stained cells in the rabbit retina and comparison with other mammalian species. *Journal of Comparative Neurology* **413**, 305–326.

MACNEIL, M.A. & MASLAND, R.H. (1998). Extreme diversity among amacrine cells: Implications for function. *Neuron* **20**, 971–982.

MASLAND, R.H. (2001). The fundamental plan of the retina. *Nature Neuroscience* **4**, 877–886.

NELSON, R. (1982). AII amacrine cells quicken time course of rod signals in the cat retina. *Journal of Neurophysiology* **47**, 928–947.

PERRY, V.H. & WALKER, M. (1980). Amacrine cells, displaced amacrine cells and interplexiform cells in the retina of the rat. *Proceedings of the Royal Society (London) B* **208**, 415–431.

POURCHO, R.G. & GOEBEL, D.J. (1987). A combined Golgi and autoradiographic study of 3H-glycine-accumulating cone bipolar cells in the cat retina. *Journal of Neuroscience* **7**, 1178–1188.

POURCHO, R.G. & OWCZARZAK, M.T. (1991). Glycine receptor immunoreactivity is localized at amacrine synapses in cat retina. *Visual Neuroscience* **7**, 611–618.

RAPER, J.A. (2000). Semaphorins and their receptors in vertebrates and invertebrates. *Current Opinion in Neurobiology* **10**, 88–94.

RODIECK, R.W. & BRENING, R.K. (1983). Retinal ganglion cells: Properties, types, genera, pathways and trans-species comparisons. *Brain Behavior and Evolution* **23**, 121–164.

SANDELL, J.H. & MASLAND, R.H. (1986). A system of indoleamine-accumulating neurons in the rabbit retina. *Journal of Neuroscience* **6**, 3331–3347.

STERLING, P. (2004). How retinal circuits optimize the transfer of visual information. In *The Visual Neurosciences*, eds. CHALUPA, L.M. & WERNER, J.S., pp. 243–268. Cambridge, MA: MIT Press.

STRETTOI, E. & MASLAND, R.H. (1996). The number of unidentified amacrine cells in the mammalian retina. *Proceedings of the National Academy of Sciences USA* **93**, 14906–14911.

TAUCHI, M. & MASLAND, R.H. (1984). The shape and arrangement of the cholinergic neurons in the rabbit retina. *Proceedings of the Royal Society (London) B* **223**, 101–119.

VANEY, D.I. (1984). "Coronate" amacrine cells in the rabbit retina have the 'starburst' dendritic morphology. *Proceedings of the Royal Society (London) B* **220**, 501–508.

VANEY, D.I. (1985). The morphology and topographic distribution of AII amacrine cells in the cat retina. *Proceedings of the Royal Society (London) B* **224**, 475–488.

VANEY, D.I. (1990). The mosaic of amacrine cells in mammalian retina. In *Progress in Retinal Research*, eds. OSBORNE, N. & CHADER, J., pp. 49–100. Oxford, UK: Pergamon Press.

VANEY, D.I. (1991). Many diverse types of retinal neurons show tracer coupling when injected with biocytin or Neurobiotin. *Neuroscience Letters* **125**, 187–190.

VANEY, D.I., PEICHL, L. & BOYCOTT, B.B. (1981). Matching populations of amacrine cells in the inner nuclear and ganglion cell layers of the rabbit retina. *Journal of Comparative Neurology* **199**, 373–391.

VARDI, N. & AUERBACH, P. (1995). Specific cell types in cat retina express different forms of glutamic acid decarboxylase. *Journal of Comparative Neurology* **351**, 374–384.

VÖLGYI, B., XIN, D., AMARILLO, Y. & BLOOMFIELD, S.A. (2001). Morphology and physiology of the polyaxonal amacrine cells in the rabbit retina. *Journal of Comparative Neurology* **440**, 109–125.

WEST, R.W. (1976). Light and electron microscopy of the ground squirrel retina: Functional considerations. *Journal of Comparative Neurology* **168**, 355–378.

WRIGHT, L.L. & VANEY, D.I. (2000). The fountain amacrine cells of the rabbit retina. *Visual Neuroscience* **16**, 1145R–1156R.

ZHANG, J., LI, W., TREXLER, E.B. & MASSEY, S.C. (2002). Confocal analysis of reciprocal feedback at rod bipolar terminals in the rabbit retina. *Journal of Neuroscience* **22**, 10871–10882.